Several different ways to increase the accuracy of the numerical solution of the first order wave equation

Murodil Madaliev[1], *Jahongir* Orzimatov[1]*, Zokhidjon* Abdulkhaev[1*]*, Olimjon* Esonov[1], and *Mirzohid* Mirzaraximov[1]

[1]Fergana Polytechnic Institute, house 86, Fergana Str., 150107 Fergana, Uzbekistan

Abstract. The article presents several different ways to increase the accuracy of the numerical solution of differential equations. The comparison of schemes with different accuracy for the first order wave equation problem is presented. The schemes of the first order of upwind scheme, the second order of accuracy of McCormack, the third order of accuracy of Warming–Cutler–Lomax, and the scheme of the fourth order of accuracy of Abarbanel–Gotlieb–Turkel were applied. The condensed computational grids for the McCormack scheme are used, and the results using an adaptive grid for the McCormack scheme were compared.

1 Introduction

Mathematical modeling, as one of the ways to obtain new knowledge, is today one of the main research methods in various fields of natural science. The movement of gas in a wind tunnel, the propagation of tsunami waves, the spread of plasma in a trap, weather changes and other numerous phenomena in science and technology are described by various mathematical models represented as integral or partial differential equations. Modern computational algorithms make it possible to solve these systems of equations with sufficient accuracy in two-dimensional and three-dimensional approximations when solving various classes of problems [1-2], considering real geometries and non-stationarity of the process [3]. Further progress in the development of numerical methods is associated with the development of new numerical algorithms and an increase in the speed and power of modern computer technology [1], [4-8].

   Modern problems of mathematical physics impose various requirements on the applied numerical algorithms, the main of which are
- high order of approximation (provides a more accurate solution on fairly coarse grids);
- the stability of the algorithms, which makes it possible to carry out calculations with large time steps);
- conservativeness (correct resolution of discontinuous solutions);
- monotonicity (absence of oscillations in areas of large gradients);
- efficiency (as minimization of the number of arithmetic operations per grid node);

---

* Corresponding author: zohidjon20.06@gmail.com

- universality of algorithms (the possibility of their extension to multidimensional (2D, 3D problems);
- adaptation of algorithms to irregular or unstructured grids;
- the possibility of parallelization of calculations (when using several computing processors - cores) [9].

Various finite-difference schemes that can be used to solve the simplest model equations will be presented. We will confine ourselves to consideration of the wave equation of the first order. These equations are called model equations because they are used to study the properties of solutions to more complex partial differential equations. Thus, the heat equation can be considered as a model for other partial differential equations, e.g., the Navier-Stokes equations [10-12]. All considered model equations have analytical solutions under certain boundary and initial conditions. Knowing these solutions, it is easy to evaluate and compare the various finite-difference methods used to solve more complex partial differential equations. Of the many existing finite-difference methods for solving partial differential equations, this article describes mainly those methods that have properties characteristic of a whole class of similar methods. Some finite-difference methods useful for solving equations are not given, since they are like those described by Khakimzyanov and Chernyy [12] and Anderson et al. [13].

As one of the most popular methods of numerical solution for partial differential equations, the finite-difference method (FDM) has been widely utilized in seismic modeling [15-18] and migration [19-21]. To improve the accuracy and stability of a FDM in numerical modeling, many methods have been developed, including difference schemes of variable grid [22, 23], irregular grid [24, 25], standard staggered grid [26, 27], rotated staggered grid [28], variable time step [29], and implicit methods [30].

Since the efficiency of an algorithm must consider the central processing unit demands and the memory demands, a desirable algorithm must balance input/output and memory needs. In general, a lower-order finite-difference algorithm uses a shorter operator but requires more grid points; while a higher-order finite-difference algorithm uses a longer operator but requires fewer grids. One is the economy achieved in storage requirements at no extra cost of total computational time, which make it possible to compute larger models or higher frequency solutions within the available core memory on the computer. To increase efficiency and accuracy of such modeling, Crase presented an elastic finite-difference scheme with arbitrary-order accuracy in both space and time [31]. Liu developed finite-difference formulas with any even-order accuracy for any order derivative, which were used to simulate elastic wave propagation in two-phase anisotropic media [32, 33].

In this article, we select equation (1) as a model equation, which we will call the one-dimensional wave equation of the first order, or simply the wave equation. The one-dimensional wave equation is a linear hyperbolic equation describing the propagation of a wave with a velocity c along the x-axis. In elementary form, it models nonlinear equations describing gas-dynamic flows [34].

$$\frac{\partial u}{\partial t} + c\frac{\partial u}{\partial x} = 0, c > 0 \tag{1}$$

Exact analytical solution of equation (1) with initial data

$$u(x, 0) = F(x), \qquad -\infty < x < \infty,$$

has the form

$$u(x, t) = F(x - ct).$$

The discussion of the article consists of three parts. In the first part, we compare schemes with different accuracy for the first order wave equation problem. In the second part, we use

condensed computational grids. In the third part, we compare the results using an adaptive grid.

For comparison, the most popular finite-difference schemes were used, such as the upwind scheme, the McCormack scheme, the Warming-Cutler-Lomax scheme, and the Abarbanel-Gotlieb-Turkel scheme.

The main purpose of the article is to show ways to improve the accuracy of partial differential equations. To improve the accuracy in the article, four methods were used, 1) increase the accuracy of the algorithm, 2) increase the number of lattices meshes, 3) use condensed meshes, 4) use adaptive meshes. The article shows all these ways.

2 Initial and boundary conditions

At the beginning, it is necessary to find the conditions for the existence of a weak solutions of the wave equation (1), i.e., the necessary conditions for the existence of a solution with a discontinuity, as shown in Fig. 1.
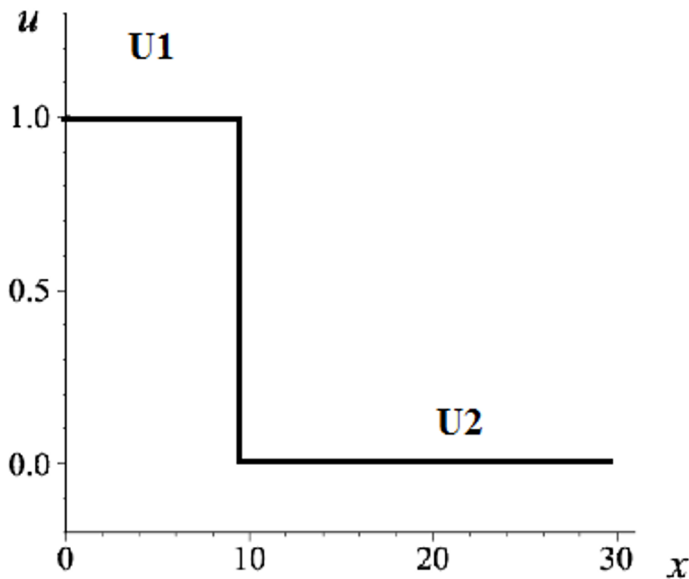
Fig. 1. A typical problem of discontinuity propagation.

Let the initial function be discontinuous at the point $x \in (0, l]$.

$$u_0(x) = \begin{cases} u_1, x < x_0 \\ u_2, x > x_0 \end{cases} \tag{2}$$

First, we present the results of a numerical solution of this problem on a uniform grid with nodes xi = ih (i = 0, ..., N) and a step h = l/N (N = 90, 450) for the following values of the input data:

$$l = 30, x_0 = 10, c = 1, u_1 = 1, u_2 = 0$$

For the stability of numerical schemes, the Courant-Friedrichs-Levy criterion (CFL-criterion) was used. The CFL-criterion is a necessary condition for the stability of the explicit numerical solution of partial differential equations. Consequently, in many computer

simulations the time step must be less than a certain value or the results will be incorrect. The physical criterion of CFL means that a liquid particle in one time step should not move more than one spatial step. Or, in other words, the computational scheme cannot correctly calculate the propagation of a physical disturbance, which moves faster than the computational scheme allows "tracking", that is, one step in space for one step in time.

$$|u|\frac{\Delta t}{\Delta x} \leq C$$

where Δt is a time step, Δx is a x-axes distance step, the constant C = 1 depends on the equation (1), but does not depend on Δt and Δx. In all numerical experiments, the time step was specified by the formula

$$\Delta t = k\frac{h}{c}$$

where k is the safety factor, which in the calculations was assumed to be 0.1, which ensured the fulfillment of the stability conditions (CFL-criterion) with a margin.

3 Description of the schemes

3.1 Upwind scheme

A simple explicit scheme (Euler's method) [34] can be made stable if, when approximating the spatial derivative, one uses backward differences rather than forward differences in cases where the wave velocity c is positive. If the wave velocity is negative, then the stability of the circuit is ensured by using forward differences. This issue was considered in more detail by Anderson et al. [14] when describing the method of splitting matrix coefficients. When differences are used backwards, the difference equations take the form [35, 36]:

$$\frac{u_i^{n+1} - u_i^n}{\Delta t} + c\frac{u_i^n - u_{i-1}^n}{\Delta x} = 0,$$

$$u_i^{n+1} = u_i^n - c\frac{\Delta t}{\Delta x}(u_i^n - u_{i-1}^n), c > 0. \tag{3}$$

This difference scheme has the first order of accuracy with an approximation error of $O(\Delta t, \Delta x)$. It follows from the Neumann stability condition that the circuit is stable for $(\Delta t/\Delta x) \leq 1$[37].

3.2 McCormack's scheme

The McCormack method[38] is widely used to solve the equations of gas dynamics. It is especially useful for solving non-linear partial differential equations. Applying the explicit predictor-corrector method to the linear wave equation, we obtain the following difference scheme:

Predictor

$$\frac{\overline{u_i^{n+1}} - u_i^n}{\Delta t} + c\frac{u_{i+1}^n - u_i^n}{\Delta x} = 0,$$

$$\overline{u_i^{n+1}} = u_i^n - c\frac{\Delta t}{\Delta x}(u_{i+1}^n - u_i^n). \tag{4}$$

Corrector

$$\frac{u_i^{n+1} - (u_i^n + \overline{u_i^{n+1}})/2}{\Delta t/2} + c\frac{u_i^n - u_{i-1}^n}{\Delta x} = 0,$$

$$u_i^{n+1} = \left(u_i^n + \overline{u_i^{n+1}} - c\frac{\Delta t}{\Delta x}\left(\overline{u_i^{n+1}} - \overline{u_{i-1}^{n+1}}\right)\right), \tag{5}$$

$$O((\Delta t)^2, (\Delta x)^2)$$

Initially (predictor) is an estimate of the $\overline{u_i^{n+1}}$ value at the n+1-th time step, and then (corrector) is determined by the final value u_i^n at the n+1-th time step. Note that in the predictors, the derivative $\partial u/\partial x$ of the input is approximated by direct differences, while in the corrector, by inverse differences. It is possible to do the opposite, which can be useful in solving some problems. Such problems include problems with moving discontinuities. This scheme is stable at $c\Delta t/\Delta x \le 1$.

3.3 Warming-Cutler-Lomax scheme

Warming et al.[39] proposed a method of the third order of accuracy, which at the first two time steps coincides with the McCormack method and at the third with the Rusanov method:

Step 1

$$\frac{\overline{u_i^{n+1}} - u_i^n}{\Delta t} + c\frac{2}{3}\left(\frac{u_{i+1}^n - u_i^n}{\Delta x}\right) = 0,$$

$$\overline{u_i^{n+1}} = u_i^n - c\frac{2}{3}\frac{\Delta t}{\Delta x}(u_{i+1}^n - u_i^n), \tag{6}$$

Step 2

$$\overline{\overline{u_i^{n+1}}} = \left(u_i^n + \overline{u_i^{n+1}} - c\frac{2}{3}\frac{\Delta t}{\Delta x}\left(\overline{u_i^{n+1}} - \overline{u_{i-1}^{n+1}}\right)\right),$$

$$O((\Delta t)^2, (\Delta x)^2). \tag{7}$$

Step 3

$$u_i^{n+1} = u_i^n - \frac{1}{24}c\frac{\Delta t}{\Delta x}(-2u_{i+2}^n + 7u_{i+1}^n - 7u_{i-1}^n + 2u_{i-2}^n) - \frac{3}{8}c\frac{\Delta t}{\Delta x}\left(\overline{\overline{u_{i+1}^{n+1}}} - \overline{\overline{u_{i-1}^{n+1}}}\right)$$
$$- \frac{\omega}{24}(u_{i+2}^n - 4u_{i+1}^n + 6u_i^n - 4u_{i-1}^n + u_{i-2}^n).$$

This is an explicit three-step scheme of the third order of accuracy with an approximation error $O((\Delta t)^3, (\Delta x)^3)$ that is stable at $\Delta t/\Delta x \le 0.01$, $\omega = c\Delta t/\Delta x^2 - c\Delta t/\Delta x^4$.

3.4 Abarbanel–Gotlieb–Turkel scheme

Abarbanel et al. [40] presented a four-step scheme of the fourth order of accuracy. This schema looks like this:

Step 1

$$u_{j+\frac{1}{2}}^{(1)} = \frac{1}{2}\left(u_{j+1}^n + u_j^n\right) - c\frac{\Delta t}{2\Delta x}\left(u_{j+1}^n - u_j^n\right), \tag{9}$$

Step 2

$$u_j^{(2)} = \frac{1}{8}\{10u_j^n - (u_{j+1}^n + u_{j-1}^n)\} - c\frac{\Delta t}{2\Delta x}\left(u_{j+\frac{1}{2}}^{(1)} - u_{j-\frac{1}{2}}^{(1)}\right), \tag{10}$$

Step 3

$$u_{j+\frac{1}{2}}^{(3)} = \frac{1}{16}\{9(u_{j+1}^n + u_j^n) - (u_{j+2}^n + u_{j-1}^n)\}$$
$$- c\frac{\Delta t}{8\Delta x}[8(u_{j+1}^{(2)} - u_j^{(2)}) + 3(u_{j+1}^n - u_j^n) - (u_{j+2}^n - u_{j-1}^n)], \tag{11}$$

Step 4

$$u_j^{n+1} = u_j^n - c\frac{1}{96}\frac{\Delta t}{\Delta x}\left[16\left(u_{j+\frac{1}{2}}^{(3)} - u_{j-\frac{1}{2}}^{(3)}\right) + 16(u_{j+1}^{(2)} - u_{j-1}^{(2)})\right.$$
$$+ 56\left(u_{j+\frac{1}{2}}^{(1)} - u_{j-\frac{1}{2}}^{(1)}\right) - 8\left(u_{j+\frac{3}{2}}^{(1)} - u_{j-\frac{3}{2}}^{(1)}\right)\right] + u \tag{12}$$
$$* c\frac{1}{96}\frac{\Delta t}{\Delta x}[10(u_{j+1}^n - u_{j-1}^n) - (u_{j+2}^n - u_{j-2}^n)].$$

This is an explicit four-step scheme of the fourth order of accuracy with an approximation error $O((\Delta t)^4, (\Delta x)^4)$, stable at $c(\Delta t/\Delta x) \leq 1$. In Equations 8-12 at the boundary, extrapolation terms were used.

When using methods of the third and fourth order of accuracy, the increase in the accuracy of the algorithm must be compensated by the complexity of the difference scheme. This must be carefully considered when choosing a method for solving a partial differential equation.

4 Discussion

4.1 Scheme results comparison

In the first part, as mentioned above, we take the results in the uniform grid of Fig. 2 at N = 90, $\Delta x = 0.333$.
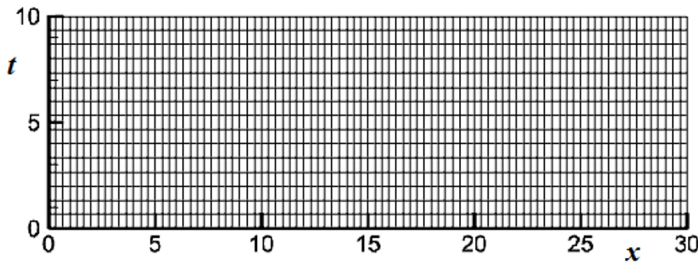

Fig. 2. Uniform mesh N = 90

The diagrams comparing circuit versus flow with exact solutions (Fig. 3 a) and b)) show that the upwind scheme does not give oscillations in the numerical solution, however, due to the first order of approximation, it is strongly "smeared" in the vicinity of the discontinuity.
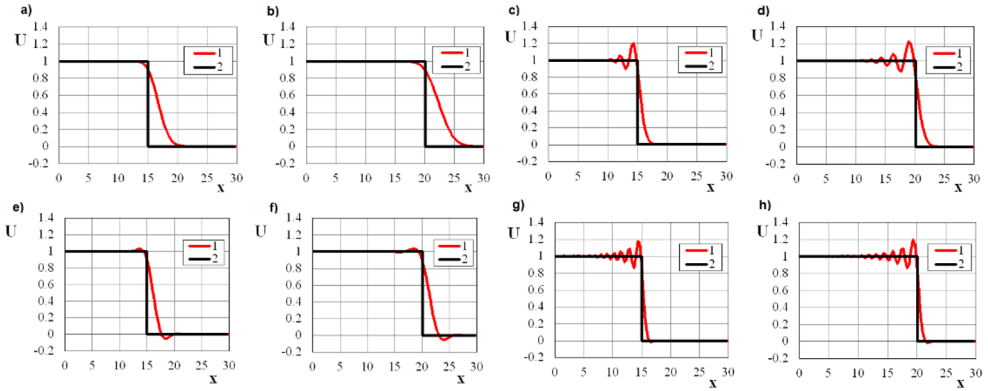
Fig. 3. Comparison of circuit results of numerical solution (1) for upwind circuit a) x=15 and b) x=20, McCormack circuit c) x=15 and d) x=20, Warming-Cutler-Lomax circuit e) x=15 and f) x=20, Abarbanel–Gottlieb–Turkel scheme g) x=15 and h) x=20 with exact solutions (2).

The McCormack scheme gives oscillations in the numerical solution; however, it gives better results than the upstream scheme (Fig. 3 c) and d)). The Warming - Cutler – Lomax scheme against the flow is strongly "smeared" in the vicinity of the discontinuity (Fig. 3 e) and f)). Oscillations in the numerical solution also exist, but not like the McCormack scheme.

It can be seen from Fig. 3 g) and h) that the Abarbanel–Gottlieb–Turkel scheme of oscillations increased in the numerical solution, but "smeared out" in the vicinity of the discontinuity decreased. The closest results to exact solutions give the McCormack scheme and the Abarbanel–Gottlieb–Turkel scheme (Fig. 4).
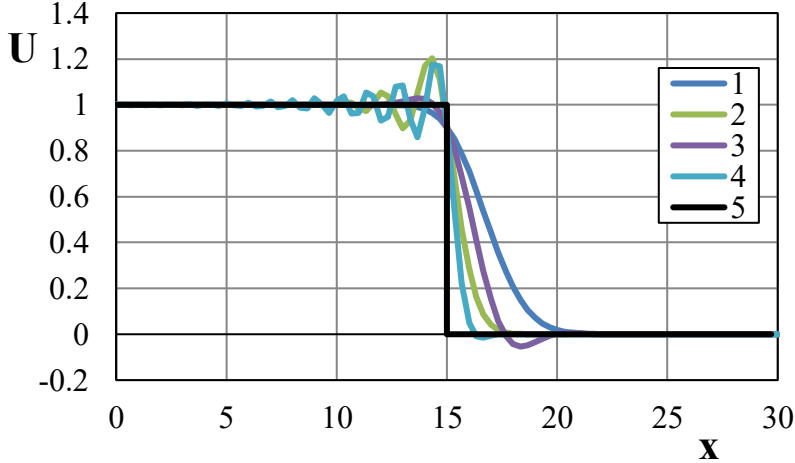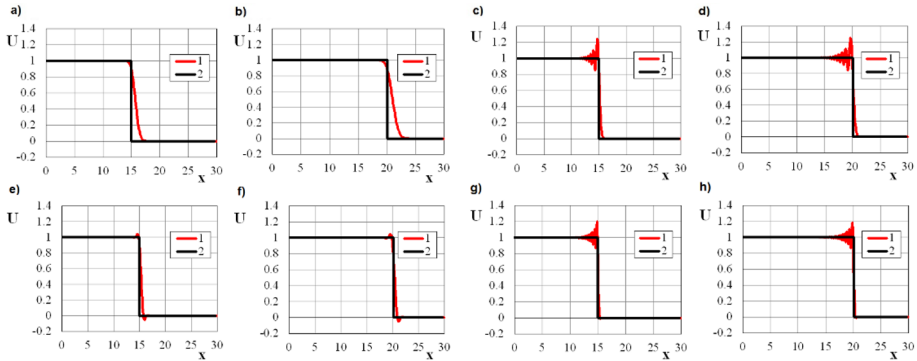

Fig. 4. Comparison of the results of various schemes with exact solutions: 1) upwind scheme, 2) McCormack scheme, 3) Warming-Cutler-Lomax scheme, 4) Abarbanel-Gotlieb-Turkel scheme, 5) exact solution.

To improve the accuracy of the solution, it is necessary to increase the number of grids in the computational domain, so now let's look at the results on a uniform grid at N = 450 and $\Delta x = 0.0666$ (Fig. 5).
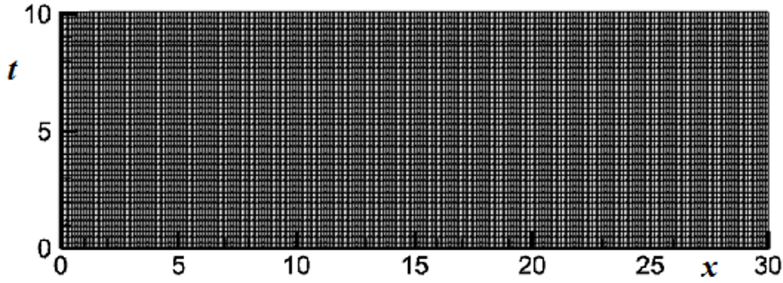
Fig. 5. Uniform mesh N = 450.

Fig. 6. Comparison of circuit results of numerical solution (1) for upwind circuit a) x=15 and b) x=20, McCormack circuit c) x=15 and d) x=20, Warming-Cutler-Lomax circuit e) x=15 and f) x=20, Abarbanel–Gottlieb–Turkel scheme g) x=15 and h) x=20 with exact solutions (2).

The refining of the grid cause that the "smearing" of the numerical solution decreases, and the discontinuity is transmitted more accurately, while the oscillations in the numerical solution increase, and the calculation time also increases (Fig. 6 and 7).
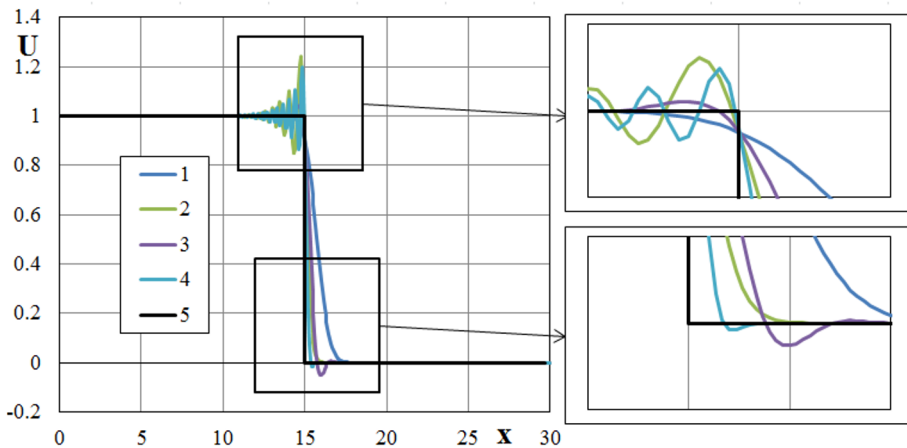
Fig. 7. Comparison of the results of various schemes with exact solutions in case of x = 15: 1) upwind scheme, 2) McCormack scheme, 3) Warming-Cutler-Lomax scheme, 4) Abarbanel-Gottlieb-Turkel scheme, 5) exact solution.

4.2 The condensed computational grids

Now we use mesh thickening with coordinate transformation $x \to \xi$ [41]-[42].

$$e \tag{13}$$

Here

$$B_x = \frac{1}{2\tau_x} \ln\left[\frac{1 + (e^{\tau_x} - 1)(x_c/l)}{1 + (e^{-\tau_x} - 1)(x_c/l)}\right], 0 < \tau_x < \infty, x_c = 15. \tag{14}$$

Where τx is the tension parameter, varying from zero to large values. Values τx = 2 were used. With this transformation, the spatial steps varied within the limits at τx = 2, 0.28 < Δx < 0.43, τx = 5, 0.13 < Δx < 0.82 and τx = 10, 0.022 < Δx < 1.57 (Fig. 8).

After the transformation, the system equation (1) changes as follows

$$\frac{\partial u}{\partial t} + c\frac{\partial \xi}{\partial x}\frac{\partial u}{\partial \xi} = 0. \tag{15}$$

(a)

(b)

(c)
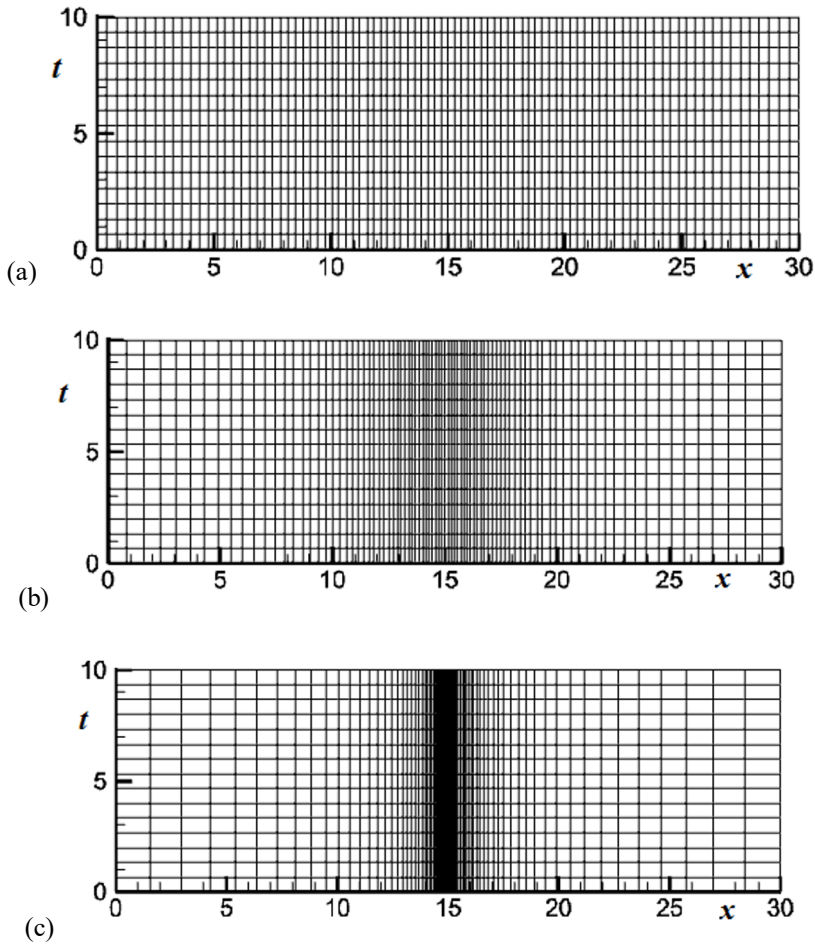
Fig. 8. Change the tension parameter. a) τx = 2, b) τx = 5, c) τx = 10.

As you can see from the pictures above, the result obtained by the McCormack scheme is close to the exact solution. Usually, for most applications, methods of the second order of accuracy can be obtained with sufficient accuracy. therefore, in the following sections, we have used only the McCormack schema. From Fig. 9a is visible in the central part where the grid is thickened, the accuracy increases, and at x = 20 the result deteriorates sharply.
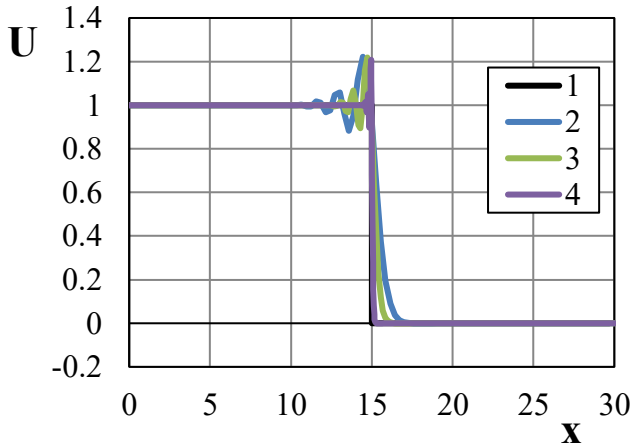
(a)
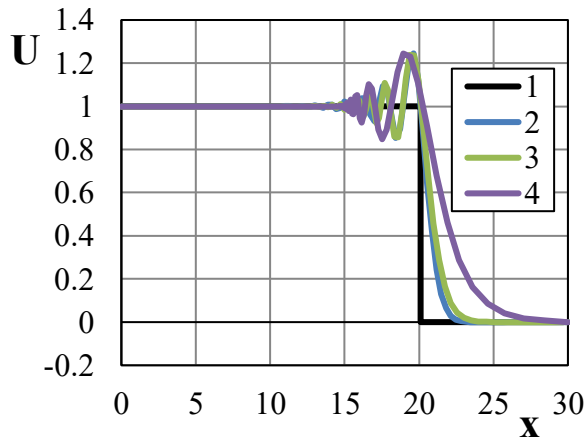
(b)

Fig. 9. Comparison of the results of various condensations of the McCormack scheme for a) x = 15, b) x = 20 with 1) exact solution, 2) $\tau x = 2$, 3) $\tau x = 5$, 4) $\tau x = 10$.

4.3 An adaptive grid

In non-stationary problems, features of the solution such as zones with large gradients shift over time, change their position, so the non-uniform grid tracking them must be mobile [44]-[45]. Such moving grids that adapt to the solution and consider the change in the solution over time are called dynamically adaptive.

Now, we will assume that there exists some smooth non-degenerate coordinate transformation

$$x = x(\xi, t), x(0, t) = 0, x(1, t) = l. \tag{16}$$

According to the law, in problem (1) we pass to independent variables ξ, t. Let $v(\xi, t) = u(x(\xi, t), t)$, i.e., the function v takes the same value at the point (ξ, t) as the function u takes at the point (x, t), corresponding to the point (ξ, t) under the mapping conditions (16). Then, according to the rule of differentiation of a complex function, we obtain that

$$\frac{\partial v}{\partial t} + \frac{c - \frac{\partial x}{\partial t}}{\frac{\partial x}{\partial \xi}} \frac{\partial v}{\partial \xi} = 0. \tag{17}$$

Let us describe an algorithm for solving the resulting difference problem on a moving grid. First, the non-uniform grid $xj0$ is constructed by the equidistributional method on the initial time layer, i.e., for n = 0. The essence of the equidistributional method is that from the set of possible mappings of the equation (16) one is selected that, at t = 0, is the solution to the boundary value problem

$$\frac{\partial}{\partial \xi}\left(\omega(x, 0)\frac{\partial x}{\partial \xi}\right) = 0, x(0,0) = 0, x(1,0) = l. \tag{18}$$

where $\omega(x,t)$ is a given control function. For definiteness, we will further assume that the control function is given in the form

$$\omega(x, t) = 1 + \alpha \left|\frac{\partial u}{\partial t}(x, t)\right|. \tag{19}$$

where α is the parameter of the control function.

To calculate the coordinates $xn+1$, we will use the finite-difference analogue of the equation

$$\frac{\partial}{\partial \xi}\left(\omega(x, t)\frac{\partial x}{\partial \xi}\right) = \beta \frac{\partial x}{\partial t}. \tag{20}$$

Where β is a positive parameter selected experimentally to reduce the oscillations of the grid node trajectories. For small β, the influence of this term is insignificant, and for large values of the parameter β, the node displacements decrease, and the grid becomes "slow-moving". Such a change in the grid is presented in Fig. 10, for the case of parameters $\alpha = 5$ and $\beta = 10$.
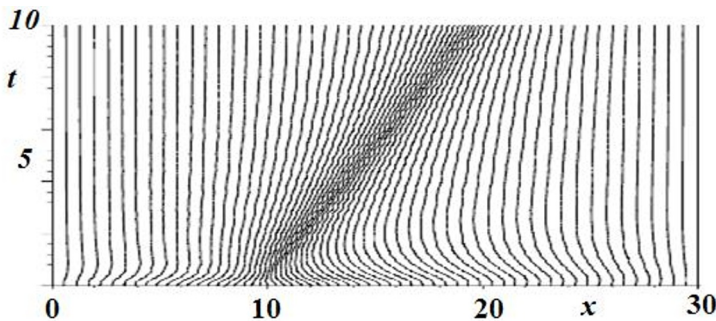

Fig. 10. Change in the computational grid with a change in time.

In the adaptive version, the McCormack scheme was also used. It can be seen from Fig. 11 that the use of the adaptive grid does not eliminate oscillations in the numerical solution, but the position of the jump is transmitted better than when using a uniform grid with the same number of nodes in Fig. 3c and Fig. 3d.
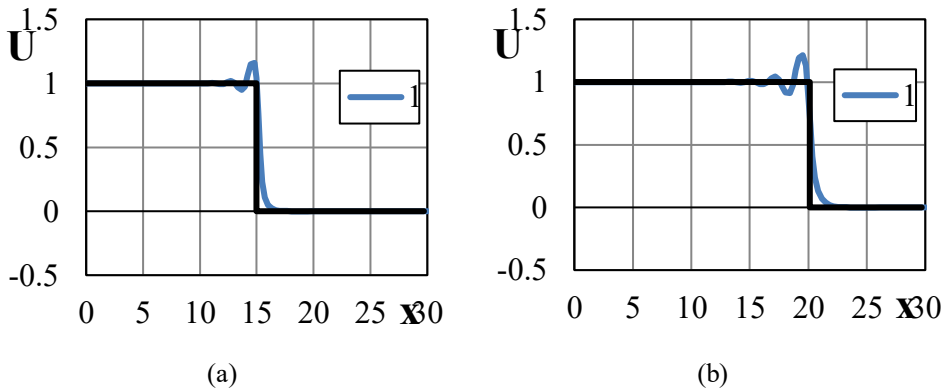
Fig. 11. Comparison of McCormack's scheme for a) x = 15 and b) x = 20 in 1) adaptive grid and 2) exact solutions.

Based on the comparison graphs of the McCormack scheme in simple, condensed ($\tau x = 5$) and adaptive grids with exact solutions (Fig. 12 a-b) it's visible that the result when using the adaptive oscillation grid is reduced and the gap is described more accurately at all.
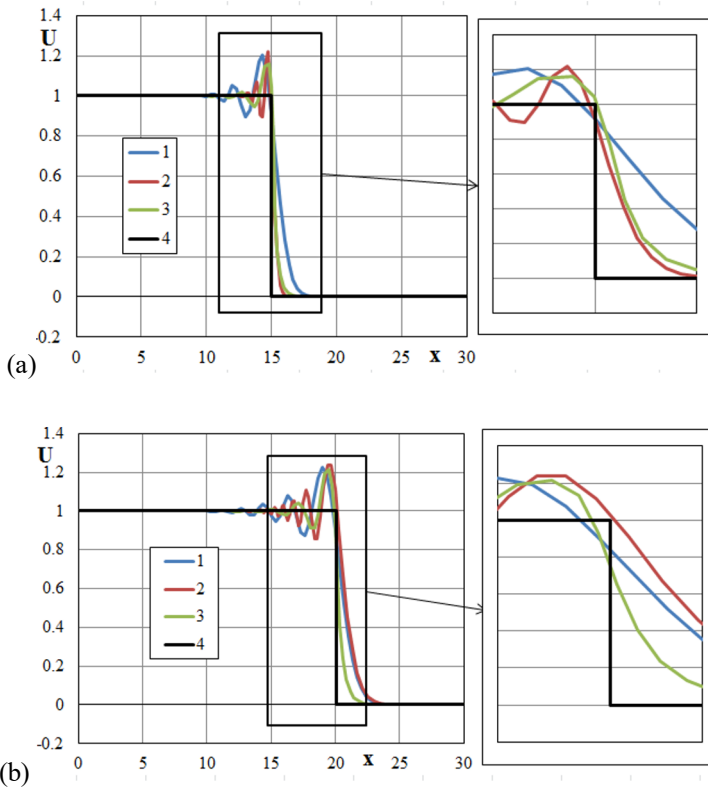
Fig. 12. Comparisons of McCormack's scheme when a) x = 15 and b) x = 20 in 1) simple, 2) condensed ($\tau x = 5$), 3) adaptive grids and 4) exact solutions.

All these methods for improving the accuracy were used for the problem of separated flow around a square cylinder in turbulent molasses. To solve this problem, the two-fluid model of turbulence by Z.M. Malikov[46] was used. The physical scheme of the flow and

the boundaries of the computational domain are shown in Fig. 13. Experimental results were taken by Lin et al [47-50]. The input constant velocity U0 was 0.535 m/s, giving a Reynolds number $\mathrm{Re}_D = U_0 D / v$ of 21400.
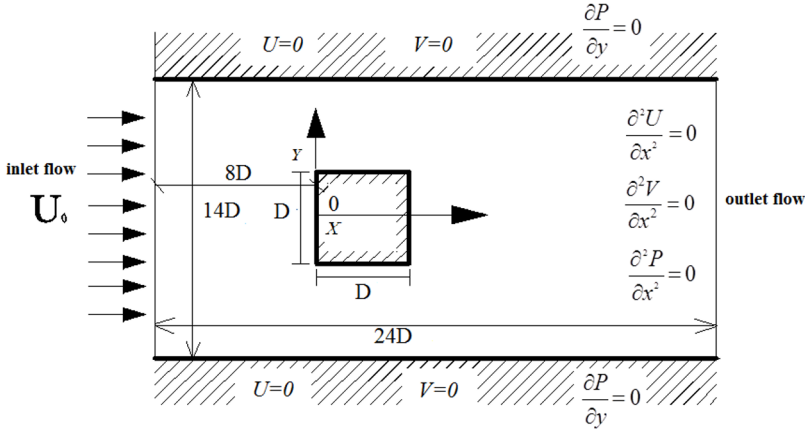

**Fig. 13.** Schematic diagram of the transverse flow around a square cylinder

The main equations for studying the problem posed are the hydrodynamic equations of the two-fluid model[43] for an incompressible medium.

$$
\begin{cases}
\dfrac{\partial V_j}{\partial x_j} = 0, \\[2ex]
\dfrac{\partial V_i}{\partial t} + \dfrac{\partial V_j V_i}{\partial x_j} + \dfrac{\partial p}{\rho \partial x_i} = \dfrac{\partial}{\partial x_j}\left[v\left(\dfrac{\partial V_i}{\partial x_j} + \dfrac{\partial V_j}{\partial x_i}\right) - \vartheta_j \vartheta_i \right], \\[2ex]
\dfrac{\partial \vartheta_i}{\partial t} + \dfrac{\partial V_j \vartheta_i}{\partial x_j} = -\vartheta_j \dfrac{\partial V_i}{\partial x_j} + \dfrac{\partial}{\partial x_j}\left[v_{ji}\left(\dfrac{\partial V_i}{\partial x_j} + \dfrac{\partial V_j}{\partial x_i}\right)\right] + F_{si} + F_{fi}, \\[2ex]
v_{ji} = 3v + 2\left|\dfrac{\vartheta_i \vartheta_j}{def(\vec{V})}\right| \quad i \neq j, \qquad v_{ii} = 3v + \dfrac{\vartheta_k \vartheta_k \left|\dfrac{\partial \vartheta_k}{\partial x_k}\right|}{def(\vec{V})\left|\dfrac{\partial \vartheta_j}{\partial x_j}\right|}, \\[2ex]
\vec{F}_f = -K_f \vec{\vartheta}, \qquad \vec{F}_s = C_s rot\vec{V} \times \vec{\vartheta}.
\end{cases}
\tag{21}
$$

In the given system of equations, is the component of the average flow velocity, ϑ_i is the component of the relative velocity, v_{ji} are the effective molar viscosities, P is the pressure, is the density of the medium, is the molecular viscosity, is the coefficient of friction, C_s is the coefficient at the Saffman force, is the strain rate, determined as follows:

The remaining value was presented in the article[46]. In this work, for the difference approximation of the initial equations, the implicit McCormack's scheme was used and the SIMPLE control volume method was applied.

On fig. 14 represents the dimensionless time-averaged flow velocity along the centerline of the area represented by the simulation results and can be used to determine the length of the separation or recirculation zone behind a square block.
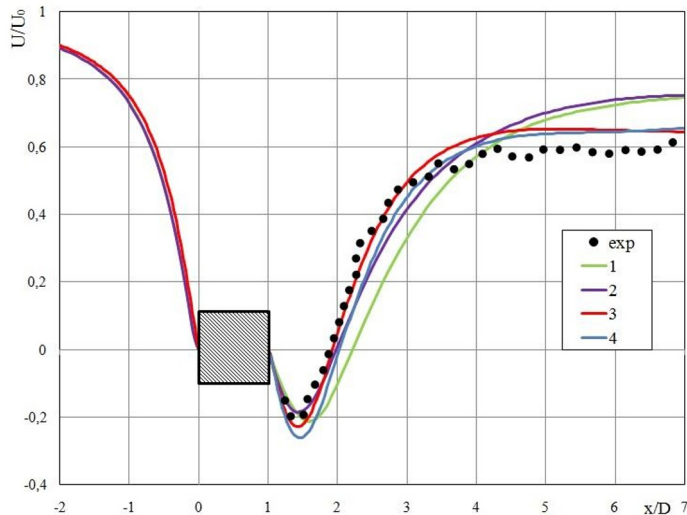
Fig.14. Dimensionless time-averaged flow velocity along the centerline. ● - experimental results, 1 - numerical results of the model with a coarse computational grid (300x300 grid), 2 - with a fine grid (600x600 grid), 3 - with a condensed grid (300x300 grid), 4 - adaptive grids (160x120 grid)

From Fig. 14 it can be seen that with an increase in the number of lattice grids, the result approaches the experiment. When using mesh density in the central parts of the square, the result fits the experiment very well. When using an adaptive movable computational grid with a size of 160x120 on the concept of the equidistribution method. It can be seen from the study that a good result can be obtained with a very small number of grids using an adaptive grid.

5 Conclusions

To improve the accuracy of the result, the accuracy of the circuit can be increased, but it leads to the complexity of the circuit. In case of the increase the number of grid steps, the calculation time will also increase. Therefore, it is advisable to use mesh compression or adaptive meshes. To solve stationary problems when the position of the discontinuity does not change, grid compression can be used. If the task is non-stationary, that is, the position of the gap changes, an adaptive grid must be used. And also in the article all these methods were used for the problem of turbulent flow around a square cylinder and very good numerical results were taken in the condensed mesh and in the adaptive mesh.

6 Acknowledgements

References

1. D. Griffini, M. Insinna, S. Salvadori, A. Barucci, F. Cosi, S. Pelli, G.C. Righini, On the CFD Analysis of a Stratified Taylor-Couette System Dedicated to the Fabrication of Nanosensors. Fluids, **2**, 8 (2017) https://doi.org/10.3390/fluids2010008.

2. F. Ries, Y. Li, M. Rißmann, D. Klingenberg, K. Nishad, B. Böhm, A. Dreizler, J. Janicka, A. Sadiki, Database of Near-Wall Turbulent Flow Properties of a Jet Impinging on a Solid Surface under Different Inclination Angles. Fluids, **3**, 5 (2018) https://doi.org/10.3390/fluids3010005

3. A. N. Lipatnikov, Numerical Simulations of Turbulent Combustion. Fluids, **5**, 22 (2020) https://doi.org/10.3390/fluids5010022

4. A. Arifjanov, L. Samiev, S. Yusupov, D. Khusanova, Z. Abdulkhaev, S. Tadjiboyev, *Groundwater Level Analyse In Urgench City With Using Modflow Modeling And Forecasting System*, E3S Web of Conferences, 263 (2021) https://doi.org/10.1051/e3sconf/202126303010

5. Y. K. Rashidov, K. Y. Rashidov, I. I. Mukhin, Kh. T. Suratov, J. T. Orzimatov, Sh. Sh. Karshiev, Main Reserves for Increasing the Efficiency of Solar Thermal Energy in Heat Supply Systems (Review). Appl. Sol. Energy, **55**, 91–100 (2019) https://doi.org/10.3103/S0003701X19020099

6. Y. K. Rashidov, J. T. Orzimatov, K. Y. Rashidov, Z. X. Fayziev, The Method of Hydraulic Calculation of a Heat Exchange Panel of a Solar Water-Heating Collector of a Tube–Tube Type with a Given Nonuniform Distribution of Fluid Flow Along Lifting Pipes. Appl. Sol. Energy, **56**, 30–34 (2020) https://doi.org/10.3103/S0003701X20010107.

7. A. Arifjanov, L. Samiev, Z. Abdulkhaev, D. Abduraimova, S. Yusupov, T. Kaletová, Model of urban groundwater level management in drainage systems. Acta Hydrol. Slovaca, **23(2)**, 172–179 (2022) doi: 10.31577/ahs-2022-0023.02.0019.

8. V.M. Kovenya, Difference methods for solving multidimensional problems. Izd. Novosib. univ., Novosib (2004)

9. D. Anderson, J.C. Tannehill, R.H. Pletcher, R. Munipalli, V. Shankar, Computational Fluid Mechanics and Heat Transfer (4th ed.). CRC Press. (2020) https://doi.org/10.1201/9781351124027

10. N. Tabatabaei, M. Hajipour, F. Mallor, R. Örlü, R. Vinuesa, P. Schlatter, RANS Modelling of a NACA4412 Wake Using Wind Tunnel Measurements. Fluids, **7**, 153 (2022) https://doi.org/10.3390/fluids7050153

11. C. Zhang, C.P. Bounds, L. Foster, M. Uddin, Turbulence Modeling Effects on the CFD Predictions of Flow over a Detailed Full-Scale Sedan Vehicle. Fluids, **4**, 148 (2019) https://doi.org/10.3390/fluids4030148

12. D. Liu, T. Nishino, Unsteady RANS Simulations of Strong and Weak 3D Stall Cells on a 2D Pitching Aerofoil. Fluids, **4**, 40 (2019) https://doi.org/10.3390/fluids4010040

13. G. S. Khakimzyanov, S. G. Chernyy, Metody vychisleniy. Novosibirsk: CH (2014)

14. D. Anderson, J. Tannehill, R. Pletcher, Computational fluid mechanics and heat transfer, **1** (1990)

15. K. R. Kelly, R.W. Ward, S. Treitel, R.M. Alford, Synthetic seismograms: A finite-difference approach. Geophysics, **41(1)**, 2–27 (1976) https://doi.org/10.1190/1.1440605

16. B.A. Abdukarimov, A.A. Kuchkarov, Numerical Solution of the Mathematical Model of Air Flow Movement in a Solar Air Heater with a Concave Tube Abdukarimov, B.A., Kuchkarov, A.A. Applied Solar Energy (English translation of Geliotekhnika), **58(1)**, 109–115 (2022)

17. R. Bansal, M.K. Sen, Finite-difference modelling of S-wave splitting in anisotropic media. Geophys. Prospect., **56(3)**, 293–312 (2008) https://doi.org/10.1111/j.1365-2478.2007.00693.x

18. B.A. Abdukarimov, A.A. Kuchkarov, Research of Hydrodynamic Processes Occurring in Solar Air Heater Collectors with a Concave Air Duct Absorber, Applied Solar Energy (English translation of Geliotekhnika), **58(6)**, 847–853 (2022)

19. J.F. Claerbout, Imaging the earth's interior, 1 (Blackwell scientific publications Oxford, 1985)

20. G. Zhang, Y. Zhang, H. Zhou, Helical finite-difference schemes for 3-D depth migration. SEG Technical Program Expanded Abstracts, 862-865 (2000) https://doi.org/10.1190/1.1816209

21. T. W. Fei, C. L. Liner, Hybrid Fourier finite-difference 3D depth migration for anisotropic media. Geophysics, **73(2)**, 27–34 (2008) https://doi.org/10.1190/1.2828704

22. Z. Wang, G.T. Schuster, Finite-difference variable grid scheme for acoustic and elastic wave equation modeling. SEG Technical Program Expanded Abstracts 1996, Society of Exploration Geophysicists, 674–677 (1996) https://doi.org/10.1190/1.1826737

23. K. Hayashi, D.R. Burns, Variable grid finite-difference modeling including surface topography. SEG Technical Program Expanded Abstracts 1999, Society of Exploration Geophysicists, 528–531 (1999) https://doi.org/10.1190/1.1821071

24. I. Opršal, J. Zahradník, Elastic finite-difference method for irregular grids. Geophysics, **64(1)**, 240–250 (1999) https://doi.org/10.1190/1.1444520

25. J.H. Harmening, H. Devananthan, F.-J. Peitzmann, B.O. el Moctar, Aerodynamic Effects of Knitted Wire Meshes—CFD Simulations of the Flow Field and Influence on the Flow Separation of a Backward-Facing Ramp. Fluids, **7**, 370 (2022) https://doi.org/10.3390/fluids7120370.

26. R. W. Graves, Simulating seismic wave propagation in 3D elastic media using staggered-grid finite differences. Bull. Seismol. Soc. Am., **86(4)**, 1091–1106 (1996) https://doi.org/10.1785/BSSA0860041091

27. J. O. A. Robertsson, J. O. Blanch, W. W. Symes, Viscoelastic finite-difference modeling. Geophysics, **59(9)**, 1444–1456 (1994) https://doi.org/10.1190/1.1443701

28. T. Bohlen, E. H. Saenger, Accuracy of heterogeneous staggered-grid finite-difference modeling of Rayleigh waves. Geophysics, **71(4)**, 109–T115 (2006) https://doi.org/10.1190/1.2213051

29. E. Tessmer, Seismic finite-difference modeling with spatially varying time stepsFD Modeling with Varying Time Steps. Geophysics, **65(4)**, 1290–1293 (2000) https://doi.org/10.1190/1.1444820

30. H.J. Zhang, Y. Zhang, J. Sun, Implicit splitting finite difference scheme for multi-dimensional wave simulation. SEG Technical Program Expanded Abstracts, 2011-2015 (2007) https://doi.org/10.1190/1.2792885

31. E. Crase, High-order (space and time) finite-difference modeling of the elastic wave equation. SEG Technical Program Expanded Abstracts 1990, Society of Exploration Geophysicists, 987–991 (1990) https://doi.org/10.1190/1.1890407

32. L. Yang, W. Xiucheng, Finite-difference numerical modeling with even-order accuracy in two-phase anisotropic media. Appl. Geophys, **5**, 107–114 (2008) https://doi.org/10.1007/s11770-008-0014-6

33. Y. Liu, M. K. Sen, Numerical modeling of wave equation by a truncated high-order finite-difference method. Earthquake Science, **22(2)**, 205-213 (2009) doi: 10.1007/s11589-009-0205-0

34. D. Anderson, J. Tannehill, R. Pletcher, Computational fluid mechanics and heat transfer. 3rd ed. (Taylor & Francis, 2016)

35. R. F. Warming, B. J. Hyett, The modified equation approach to the stability and accuracy analysis of finite-difference methods. J. Comput. Phys., **14(2)**, 159–179 (1974) https://doi.org/10.1016/0021-9991(74)90011-4.

36. M. E. U. Madaliev, Z. E. Abdulkhaev, N. E. Toshpulatov, A. A. Sattorov, Comparison of finite-difference schemes for the first order wave equation problem. AIP Conference Proceedings, **2637(1)**, 40022 (2022) https://doi.org/10.1063/5.0119158

37. R. W. MacCormack, The effect of viscosity in hypervelocity impact cratering. J. Spacecr. Rockets, **40(5)**, 757–763 (2003) https://doi.org/10.2514/2.6901

38. R.F. Warming, P. Kutler, H. Lomax, Second-and third-order noncentered difference schemes for nonlinear hyperbolic equations. AIAA J., **11(2)**, 189–196 (1973) https://doi.org/10.2514/3.50449

39. S. Abarbanel, D. Gottlieb, E. Turkel, Difference schemes with fourth order accuracy for hyperbolic equations. SIAM J. Appl. Math., **29(2)**, 329–351 (1975) https://www.jstor.org/stable/2100485

40. A. A. Mirzoev, M. Madaliev, D. Y. Sultanbayevich, Numerical modeling of non-stationary turbulent flow with double barrier based on two liquid turbulence model. 2020 International Conference on Information Science and Communications Technologies (ICISCT), 1–7 (2020)

41. E. Son, M. Murodil, Numerical calculation of an air centrifugal separator based on the SARC turbulence model. J. Appl. Comput. Mech., **6**, 1133–1140 (2020) doi:10.22055/JACM.2020.31423.1871

42. Z. M. Malikov, M. E. Madaliev, Mathematical modeling of a turbulent flow in a centrifugal separator. Vestn. Tomsk. Gos. Univ. Mat. i Mekhanika, **71**, 121–138 (2021) https://doi.org/10.17223/19988621/71/10

43. B.Q. Dong, Z. Ye, X. Zhai, Global regularity for the 2D Boussinesq equations with temperature-dependent viscosity. Journal of Mathematical Fluid Mechanics, **22**, 1-6 (2020)

44. B.Q. Dong, J. Wu, Z. Ye, Global regularity for a 2D tropical climate model with fractional dissipation. Journal of Nonlinear Science, Apr, **15(29)**, 511-50 (2019)

45. Z. M. Malikov, M. E. Madaliev, Numerical simulation of separated flow past a square cylinder based on a two-fluid turbulence model. J. of Wind Engineering and Industrial Aerodynamics, **231**, 105171 (2022)

46. B. Abdukarimov, S. O'Tbosarov, A. Abdurazakov, *Investigation of the use of new solar air heaters for drying agricultural products* E3S Web of Conferences, **264**, 01031 (2021)

47. Z. E. Abdulkhaev, M. M. Madraximov, J. T. Orzimatov, A. M. Abdurazaqov, *Transition processes during the start-up of the pumping unit of happ*, E3S Web of Conferences, **420**, 07023 (2023)

48. A. Arifjanov, S. Jurayev, T. Qosimov, S. Xoshimov, Z. Abdulkhaev, *Investigation of the interaction of hydraulic parameters of the channel in the filtration process*, E3S Web of Conferences, **401**, 03074 (2023)

49. Z. Abdulkhaev, M. Madraximov, A. Akramov, A. Arifjanov, *Groundwater flow modeling in urban areas.* AIP Conference Proceedings, **2789(1)** (2023)

50. Z. Abdulkhaev, M. Madraximov, A. Arifjanov, N. Tashpulotov, *Optimal methods of controlling centrifugal pumps.* AIP Conference Proceedings, 2612(1) (2023)